A Sponge-Like (Almost) Universal Tile

Duane A. Bailey[1] and Feng Zhu[2]
Williams College

Abstract. We present an technique for developing a single, aperiodic (or *universal*) tile that does not overlap. We provide two examples, constructed by converting overlapping regions of Gummelt's decagon cover to interleaved regions in a porous tile. Each is a bounded, dense, sponge-like set of points in $\mathbb{R}^2$ that tiles the plane aperiodically. One tile has measure zero, the other has positive measure everywhere. Many characteristics of the decagon cover are inherited by our tilings. We also discuss how to arbitrarily adjust density of portions of the tile to, for example, support models of physical quasicrystals. A similar approach could be used to eliminate overlap in higher dimensions.

1 Introduction

Since the advent of the first aperiodic tile sets[3, 25] researchers have sought a minimal prototile set that forces a nonperiodic tiling of the plane. A number of aperiodic sets have been found, although the two-tile sets of Penrose are arguably the most studied[4, 5, 6, 9, 14, 15, 16, 17, 18, 19, 20, 21, 22, 24]. The "A tiles" of Robinson are constructed by cutting Penrose's kites and darts along their medial lines; their manipulation is often more convenient where inflation and deflation is to be studied. Still, no single aperiodic tile (here, a *universal* tile) has been discovered[8]. Our premise is that the study of how single nontraditional tiles (shapes that violate one or more rules of prototile construction) perfectly tile the plane seems likely to shed light on the nature of aperiodicity and its analogy with physical systems[12].

In 1996 Gummelt[11] identified a single decagon that *covered* the plane aperiodically. The covering process involved overlapping tiles in a small number of ways. The construction, though not a proper tiling, is appealing to physical chemists who believe that the overlap models the overlapping neighborhoods of local influence that seem necessary in the perfect growth of aperiodic physical structures (called *quasicrystals*). The decagon is the direct result of considering a theorem of Conway that suggests that a decagonal *cartwheel* patch of Penrose kites and darts obeys not only a local isomorphism property, but a stronger covering condition. While the decagon approach essentially encodes the behavior of the cartwheel cover in a single overlapping tile, each tiling has properties that are not readily apparent in the other.

Later, in 1997 Bandt and Gummelt[2] and Gelbrich[7] demonstrated that set of Penrose tiles modified to include fractal edges was sufficient to remove the local matching condition. The authors suggested, as well, that in the particular case of the Penrose tiles, the complete fractal construction was not necessary, but for aesthetic reasons, the fractal boundary is appealing. One feature of this tile is an unusual notion of an edge.

Our approach is to develop a single decagon-shaped tile with fractal interior (ie. a *sponge*) that allows mutual non-overlapping entanglement of adjacent tiles where overlap would occur in the otherwise analogous decagons of Gummelt. We present two constructions, here: a lacy tile tiles the plane densely everywhere with points almost nowhere (ie. with zero measure), and a hefty tile that tiles densely with positive measure everywhere. In both cases, a perfect tiling fails to cover all points of the plane, but our measure positive construction appears to come as nearly possible to covering the plane.

2 The Cartwheel and Decagon Covers

The efficacy of Gummelt's decagon cover depends on one crucial theorem, due to Conway:

Theorem 1 *Every tiling by Penrose kites and darts can be covered by cartwheel patches.*

---

[1]bailey@cs.williams.edu, Department of Computer Science, Williams College, Williamstown, Massachusetts 01267.

[2]feng@hbs.edu, Program in Information Technology and Management, Harvard Business School, Boston, Massachusetts 02163.

A proof of this can be found in Grünbaum and Shephard[1, 10]. It stems from the observation that every tile in the plane is a member of an ace (a dart capping two adjacent kites). The Penrose tiles enjoy a unique and invertible inflation property that allows one to uniquely compose tiles to form a tiling by τ-larger,[3] similar tiles. By inflating twice, locating the appropriate ace, and deflating twice, the theorem is made obvious. (In fact the "cartwheel" used in this paper is the result of inflating the ace twice—a *second-order cartwheel*. The theorem holds for greater even-ordered cartwheels, as well.)

In a perfect cartwheel cover of the plane there are four types of intersection between any pair of cartwheels:

1. The patches do not intersect, or

2. The patches meet edge-to-edge, intersecting in an area of measure 0, or

3. The patches overlap in a manner that covers 4 darts and 7 kites (approximately 28.14% of the area of each of the participating tiles), or

4. The patches overlap in a manner that covers 7 darts and 14 kites (approximately 54.46% of the area of each of the participating tiles).

Gummelt refers to these latter types of overlap as TYPE A and TYPE B (see Figure 1). A bit of experimentation with the cartwheel identifies 4 orientations that lead to TYPE A overlap, and one that leads to TYPE B overlap (see Figure 2). Readers may find it useful to copy these figures onto overhead transparencies and experiment with the resulting translucent patches.
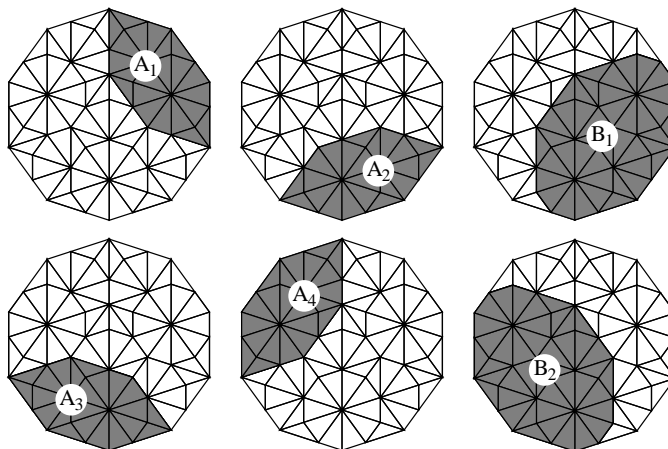

Figure 1: The six portions of the cartwheel that may overlap other cartwheel patches.

It is also interesting to note that if two tiles meet edge-to-edge then there exists a third cartwheel that (1) includes the edge and (2) consistently overlaps the first two tiles in a non-trivial TYPE A or TYPE B overlap. In this regard there are notions of cover minimization that have no analog in tilings.

By studying these overlapping areas it is possible to construct a single decagonal tile that is colored to support an overlapping rule (see Figure 3). Because these tiles overlap, there are, essentially, two edges: an external edge that defines the boundary of the decagon, and an internal edge that is the potential image of the external edge of an overlapping decagon. Two decagons are allowed to overlap if they are consistently colored on the set of overlapping points and if each segment of the decagon's external edge is covered by a segment of another decagon's internal edge. When the tiles are used to cover the plane in a manner that respects these two rules, the resulting plane exhibits no translational symmetry—that is, the cover is aperiodic (see Figure 3). The proof of aperiodicity is beyond the scope of this paper, but is fully developed by Gummelt[11].

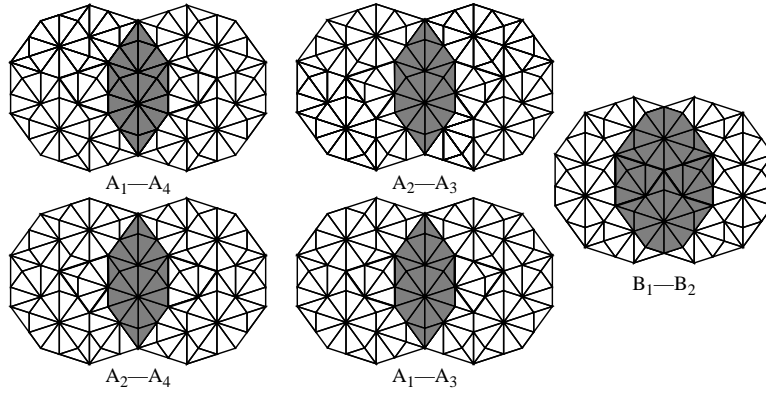[3]We use τ to represent the golden ratio $\frac{1+\sqrt{5}}{2} \approx 1.618034$.

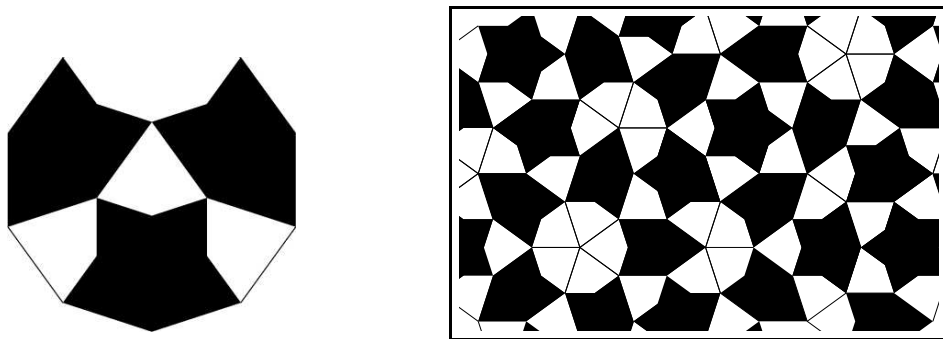Figure 2: Legal overlaps of two cartwheels.

Figure 3: Gummelt's decagon tile (left) and a patch (right).

3 The Decagon Sponge Tiles

In this section we seek to construct a decagon tile that tiles the plane densely. Our approach is similar to that of Gummelt: we begin with the cartwheel patch and develop a single tile that has tiling behavior similar to the cartwheel cover. The construction, however, violates another traditional tile concept: the tile is a decagon-bounded collection of porous, Cantor-like sets (*sponges*). Such sets do not have, in the traditional sense, any edges.

We begin by considering the potential overlap of a pair of cartwheel tiles. Figure 4 (left) depicts the regions of the cartwheel that act similarly during any of the five different TYPE A or TYPE B overlaps. In many cases two or more regions of one tile are covered by one region of another. If two points appear in different regions, they are covered by distinct regions for some overlap.
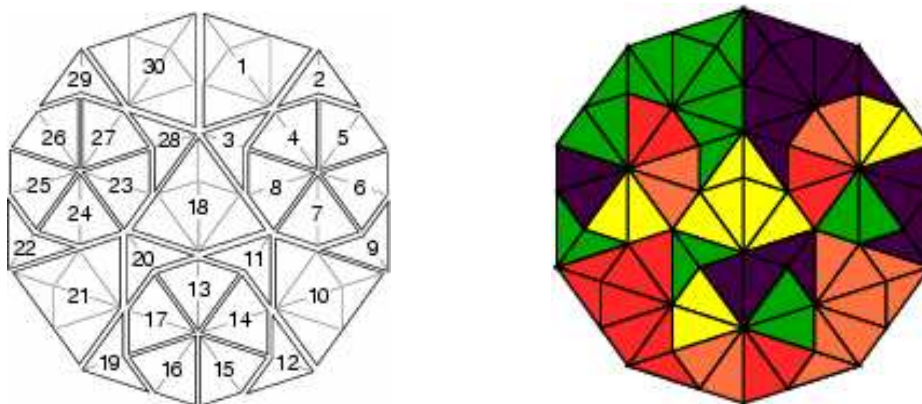

Figure 4: Left, regions of the decagon tile distinguished by overlap behavior and right, coloring of the decagon that ensures only overlaps of different colors.

For each of the five types of overlap Table 5 describes the alignment of regions in the participating tiles. We note that if two regions are mapped to one another by an overlap, they should not contain substantial sets (sets of positive measure) of coincident points; the only overlap, if any, should occur along edges.

$A_1 \leftrightarrow A_3$			$A_1 \leftrightarrow A_4$			$A_2 \leftrightarrow A_3$			$A_2 \leftrightarrow A_4$			$B_1 \leftrightarrow B_2$					
1	$\leftrightarrow$	21	1	$\leftrightarrow$	30	10	$\leftrightarrow$	21	10	$\leftrightarrow$	30	3	$\leftrightarrow$	22	12	$\leftrightarrow$	11
2	$\leftrightarrow$	20	2	$\leftrightarrow$	28	11	$\leftrightarrow$	19	11	$\leftrightarrow$	29	4	$\leftrightarrow$	25	13	$\leftrightarrow$	17
3	$\leftrightarrow$	21	3	$\leftrightarrow$	29	12	$\leftrightarrow$	20	12	$\leftrightarrow$	28	5	$\leftrightarrow$	26	14	$\leftrightarrow$	13
4	$\leftrightarrow$	17	4	$\leftrightarrow$	27	13	$\leftrightarrow$	16	13	$\leftrightarrow$	26	6	$\leftrightarrow$	27	15	$\leftrightarrow$	14
5	$\leftrightarrow$	13	5	$\leftrightarrow$	23	14	$\leftrightarrow$	17	14	$\leftrightarrow$	27	7	$\leftrightarrow$	23	16	$\leftrightarrow$	15
6	$\leftrightarrow$	14	6	$\leftrightarrow$	24	15	$\leftrightarrow$	13	15	$\leftrightarrow$	23	8	$\leftrightarrow$	24	17	$\leftrightarrow$	16
7	$\leftrightarrow$	15	7	$\leftrightarrow$	25	16	$\leftrightarrow$	14	16	$\leftrightarrow$	24	9	$\leftrightarrow$	28	18	$\leftrightarrow$	21
8	$\leftrightarrow$	16	8	$\leftrightarrow$	26	17	$\leftrightarrow$	15	17	$\leftrightarrow$	25	10	$\leftrightarrow$	18	20	$\leftrightarrow$	19
9	$\leftrightarrow$	12	9	$\leftrightarrow$	22	19	$\leftrightarrow$	12	19	$\leftrightarrow$	22	11	$\leftrightarrow$	20			

Figure 5: The association of regions under each of the 5 different overlaps.

Given this anti-dependence between regions, we seek to develop a partitioning or *coloring* of the regions such that similarly colored regions never meet in an overlap. It is possible to 5-color the regions, and we suggest a suitable coloring in Table 6. (A five-coloring is required because of the mapping of each of the three suns to the other two.) The resulting partitioning of the cartwheel is demonstrated in Figure 4 (right).

It remains, then, to develop tile shapes that (1) cover the indicated regions when no overlap occurs in that region and (2) allow the joint covering of the indicated regions when overlap does occur. It is difficult to see how a single shape can accomplish both tasks. Our approach, however, is to develop independent sets of points that are dense in the specified regions. Each "color" maps to a two-dimensional sponge that has

4

Purple	Green	Red	Orange	Yellow
1	7	8	4	5
2	14	15	10	17
3	20	19	12	18
6	22	21	16	24
9	26	27	23	
11	28			
13	29			
25	30			

Figure 6: The partitioning of regions into five colors. When two regions are matched in Table 5, they appear in different columns, here.

sufficiently small measure (or more figuratively, sufficiently high *porousness*) to allow the non-overlapping integration of differently colored sponges.

3.1 A Lacy Fixed Point Decagon Tile

To see how to develop the sponge, we recall an important property of Penrose tiles—each type of prototile covers, in the limit, a non-zero percentage of the plane. Given a convex patch of a tiling we may count the number of each type of prototile that occurs within the patch. We say that a set of prototiles is *prototile balanced* if the limit of the relative ratios of tiles is nonzero as the diameter of the patch tends toward infinity.

Theorem 2 *The Penrose tiles are prototile balanced.*

An enlightening proof of this fact is, again, found in Grünbaum and Shephard[10]. In the case of Penrose tiles, the ratio of kites to darts is τ to 1. Given this fact, we can determine that in any perfect Penrose tiling, $\frac{\tau^2}{\tau^2+1} = 72.36\%$ of the points are covered by kites, and $\frac{1}{\tau^2+1} = 27.63\%$ of the points are covered by darts.

One method for constructing a tiling is to use *tile decomposition*. One starts with a patch of tiles and decomposes each tile into self-similar prototiles, and then scales the entire structure up until the prototiles are the original size. This process is repeated and, after a countably infinite number of steps, the process produces perfect tilings. Each step develops a patch that is, asymptotically, closer to the limits required by the balancing of prototiles.

One can imagine that a similar process decomposes a region to classify points within a patch of tiles. For each tile, a single step decomposes the tile into smaller tiles,[4] but the result is not scaled up. Given a coloring of tiles, some points may be guaranteed to be colored the same after some fixed and finite number of decompositions. This "fixed point" feature may be used to generate equivalence classes of points that may be associated with colors. The appropriately colored equivalence class of points may be used in each tile of a colored region to construct a "tile" with tiling properties that are analogous to the decagon cover.

Such non-trivial equivalence classes of points exist. In fact, each class is dense in the expansion of any patch of tiles. To see this we consider the expansions of the Robinson tiles (that is, tiles that correspond to half kite and half dart tiles). Using an approach suggested by Gummelt[2], we place each tile on the complex plane and consider the transformations that identify the self-similarity of the tiles:

$$f_1(z) = (1 - \frac{z}{\tau})\omega$$

$$f_2(z) = \frac{-\overline{z}}{\tau} + \tau$$

$$f_3(z) = \frac{z}{\tau} \cdot \omega^3 + \tau$$

---

[4]Our notions of inflation and deflation map Penrose's kites and Darts tiling (*P2*) to a P2 tiling scaled up or down by factors of τ^2. A single-step inflation or deflation by τ takes kites and darts to a tiling by thin and thick rhombs which unnecessarily distracts our approach.
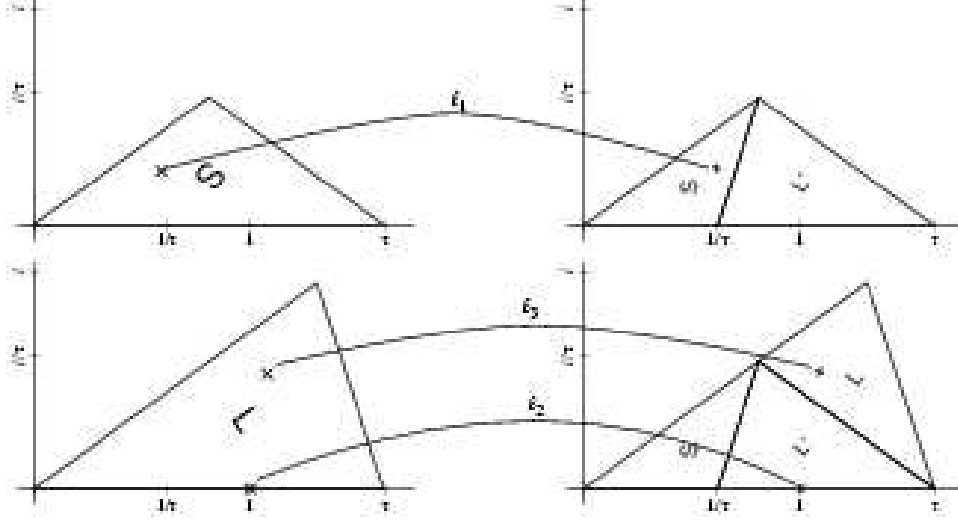
Figure 7: The self-similar relationship between Robinson's S (half dart) and L (half kite) tiles. Mappings of left-handed tiles (L' and S') are mirrored. If drawn in the complex plane, the mapping functions $f_1(z)$, $f_2(z)$, and $f_3(z)$ can be used to define the decomposition process. The functions fix the points indicated.

where $\omega = \cos(\pi/5) + i\sin(\pi/5) = \frac{\tau}{2} + i\frac{\sqrt{3-\tau}}{2}$ is the primitive 10th root of unity. The self-similar relationship between the Robinson $L = L_A$ (half kite) and $S = S_A$ (half dart) tiles is illustrated in Figure 7. We have that

$$L = f_1(S) \cup f_2(L) \cup f_3(L)$$

and

$$S = f_1(S) \cup f_2(L)$$

With such maps we may identify fixed points—points whose position is left unchanged by the transformation. Essentially, these points will always be found in the same type of prototile during decomposition:

$$F_1 = \frac{\tau\omega}{\tau + \omega} \approx (0.60, 0.25)$$

$$F_2 = (1, 0)$$

$$F_3 = \frac{1 + \tau}{\tau - \omega^3} \approx (1.09, 0.54)$$

For example, point F_1, a point of a small (S) tile will always be covered by a small tile. Unfortunately, after one decomposition, it is not possible to ensure that these fixed points are always on the interior of tiles. For example, F_2 is found on the edge of a kite; because it is on the edge, its color is not necessarily uniquely determined. However, it is clear that further decomposition of the tile must always lead to similar tiles that do not share any points of the boundary of the original.

We now develop a dense point-coloring process. First, we color regions of the Robinson S and L tiles (see Figure 8). For our purposes, we need five equivalence classes, thus we partition the two tiles into five colors, conveniently picking division lines along tile boundaries in the decomposition. After three decomposition steps, the image of each colored region contains at least one similarly colored subtile that is similarly colored; within these regions we will define colored fixed points. Since the existence of these points is independent of the context of the decomposition, each tile in any decomposed patch of tiles provides additional fixed points of each of the five colors. Because each fixed point is introduced at some finite stage of decomposition, it is clear that each of the fixed points is uniquely colored at all but a finite number of steps of decomposition. In fact, fixed points of each color reside within each open ball of the plane—they're dense in the plane. Without much effort we have
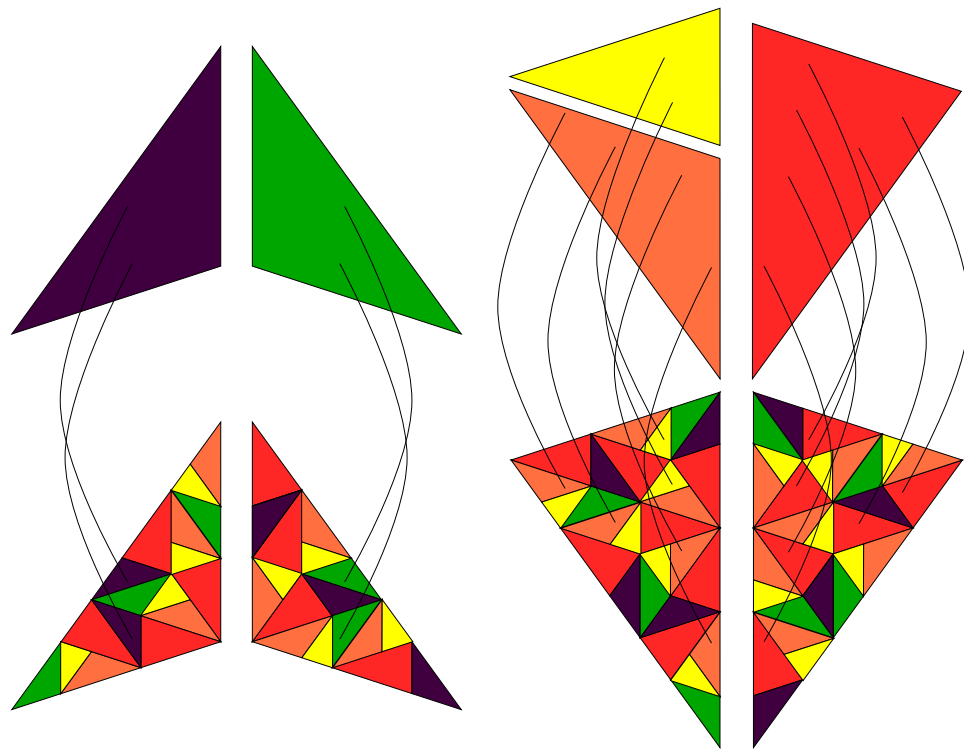
6

Figure 8: The division of tiles into five colors (above) and the tile as it is decomposed after three steps. The indicated points are fixed points of this mapping.

Theorem 3 *The coloring of eventual fixed points of the colored prototiles identifies countably many points of each color that are dense in any patch of prototiles.*

Any open ball in a tile contains at least one complete kite and one dart at some finite stage of the decomposition of the tile. These small prototiles contain at least one fixed point of each color, so the points are clearly dense. To demonstrate countability we note that we can, after every three decompositions, enumerate, for each subtile, the several newly introduced fixed points identified in Figure 8 at this stage of decomposition. It follows that over the countably infinite decomposition steps the entire collection of fixed points is, then, countable.◇

We now construct a porous decagon tile by selecting, for each colored region, the equivalence class of fixed points of the appropriate color. An approximate figure, suitable for all arguments we make here, is found in Figure 9. When two decagon tiles are brought together to overlap, the uniqueness of the decomposition of overlapping regions ensures that different colors will be represented by disjoint sets of fixed points.

Such tiles are quite porous: since the number of points that are used to represent the decagon tile are only countable, they have measure zero. This new decagon-shaped collection of points covers almost nothing, so these tiles—essentially structured dust—easily "pass through" each other. It is be necessary to introduce explicit edges in the same locations as the interior and exterior edges of the decagons of Gummelt. The matching rules, then are:

RULE 1. Each segment of an exterior edge must be covered by a segment of interior edge from some other tile, and

RULE 2. No non-edge point of a tile may be coincident with a point of another tile.

The required overlap of edges forces the alignment of tiles using TYPE A or TYPE B regions, but we must demonstrate that illegal overlaps are avoided by RULE 2.

Theorem 4 *The matching rules of the lacy decagon tile are equivalent to the decagon matching rules.*

It is fairly straightforward to see that overlap of edges required by RULE 1 allows only overlaps of TYPE A or TYPE B regions. Furthermore, when solid decagon overlaps are legitimate, the color point construction ensures that only points of differing colors appear in the same region, and consistently. Since the fixed points of the region are unambiguously colored, these point sets must be disjoint.

We now consider the overlaps of decagons that would be illegal: $A_i \leftrightarrow A_i$ $1 \leq i \leq 4$, $A_1 \leftrightarrow A_2$, $A_3 \leftrightarrow A_4$, and $B_i \leftrightarrow B_i$ $1 \leq i \leq 2$.

When the A_1 regions of two tiles are overlapped (see Figure 10), it is sufficient to see that the dart in region 9 and a dart of region 1 are brought together and are both colored purple. This brings purple fixed points of both tiles together, which is illegal under RULE 2. A similar statement argument disallows the overlap of A_4 regions of two tiles.

When the A_2 regions of two tiles are overlapped, it brings together the orange kite of region 16 with a similarly colored kite found in region 10. RULE 2 makes this illegal, as well as a similar pairing found in $A_3 \leftrightarrow A_3$ overlaps.

When an $A_1 \leftrightarrow A_2$ overlap is attempted, the left dart of region 2 is brought into alignment with a portion of the left kite of region 13, both of which are colored purple. These two shapes are consistently expanded and we have coincident purple fixed points in this region. (In Figure 8, overlap the images of the purple and orange decompositions to see this conflict.) This is illegal, under RULE 2. A similar alignment appears in the $A_3 \leftrightarrow A_4$ overlap.

We have only to consider $B_1 \leftrightarrow B_1$ and the symmetric $B_2 \leftrightarrow B_2$ alignment. Here, we note that the purple dart of region 11 is mapped to a rotated version of itself, such that the tip of one dart is aligned with the concave vertex of the other, and vise versa. Some experimentation demonstrates that after three decompositions, these regions expand in a consistent manner, bringing purple fixed points into contact with purple points of the other tile. A similar argument is made, concerning the green dart of region 20 in a $B_2 \leftrightarrow B_2$ overlap.

Since the illegal overlaps of the solid decagon are also not possible for our construction, the matching rules have the same effect as the matching rules of the solid decagon of Gummelt.◇

As a tiling mechanism this prototile could be improved. In the next section we introduce a means of selecting colored points that provides more heft to the prototile.
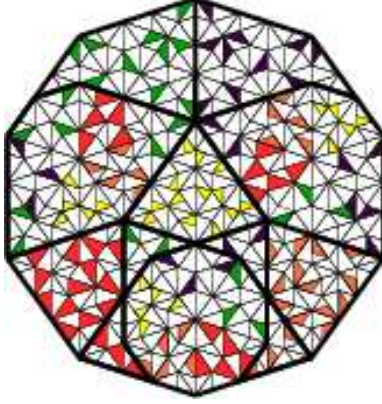
Figure 9: The first approximation to the coloring of the decagon tile. Colored tiles identify the location of the first fixed points in the region and suggest the interleaving of the tiles. Internal and external edges appear bold. Though not dense, this approximation has the same tiling properties as the ideal lacy decagon.

3.2 A Hefty Cantor-Like Decagon Tile

We now consider a general method for increasing the measure of our tile in any particular neighborhood. The method depends on the notion of constructing multiple *well-mixed* sets of points: sets that are non-zero measure and dense in the same region. We first consider the simpler problem of constructing these sets in one dimension[23], and then lift the results to two dimensions.

3.2.1 Constructing Pairs of Well-Mixed Cantor Sets

A common example from measure theory is the Cantor set on an interval of $\mathbb{R}$. We begin with the first approximation by intervals, $\mathcal{C}_0(I)$ a set containing only the interval $I = [l, r]$. We may then recursively define successive approximations, by removing the "middle thirds":

$$\mathcal{C}_i(I) = \bigcup_{[a,b] \in \mathcal{C}_{i-1}(I)} \left\{ \left[a, a + \frac{b-a}{3}\right], \left[b - \frac{b-a}{3}, b\right] \right\}$$

The Cantor set on interval I, $C(I)$, is the set of points that appear in some interval of each $\mathcal{C}_i$. This set is non-empty, for it includes all the points that appear as an endpoint of an interval at any stage. In the process of constructing this set, a large portion of the original interval is eliminated. From $\mathcal{C}_i([0,1])$, 2^i intervals of size $3^{-(i+1)}$ are removed. In the end, the measure of the amount removed from $I_0 = [0,1]$ is

$$\mu(I_0 \backslash C(I_0)) = \frac{1}{3} + \frac{2}{9} + \frac{4}{27} + \cdots = \frac{1}{3} \sum_{i=0}^{\infty} \left(\frac{2}{3}\right)^i = 1$$

suggesting the measure of the Cantor dust $C(I_0)$ is 0.

Now, consider a modified Cantor set construction that is not so aggressive about removing intervals. This version leaves behind dust, but the measure of the portion removed is much smaller, allowing the dust to accumulate. As before, $\mathcal{C}'_0(I) = \{I\}$ where $I = [l, r]$. We then define

$$\mathcal{C}'_i(I) = \bigcup_{[a,b] \in \mathcal{C}'_{i-1}(I)} \left\{ \left[a, a + \frac{(b-a)(3^i - 1)}{2 \cdot 3^i}\right], \left[b - \frac{(b-a)(3^i - 1)}{2 \cdot 3^i}, b\right] \right\}$$

The first step removes the middle third, as before. The second step removes the middle ninth of the two intervals remaining after step 1. The ith step removes the middle 3^{-i} of the remaining 2^{i-1} intervals, and so

9

A_1—A_1

A_1—A_2
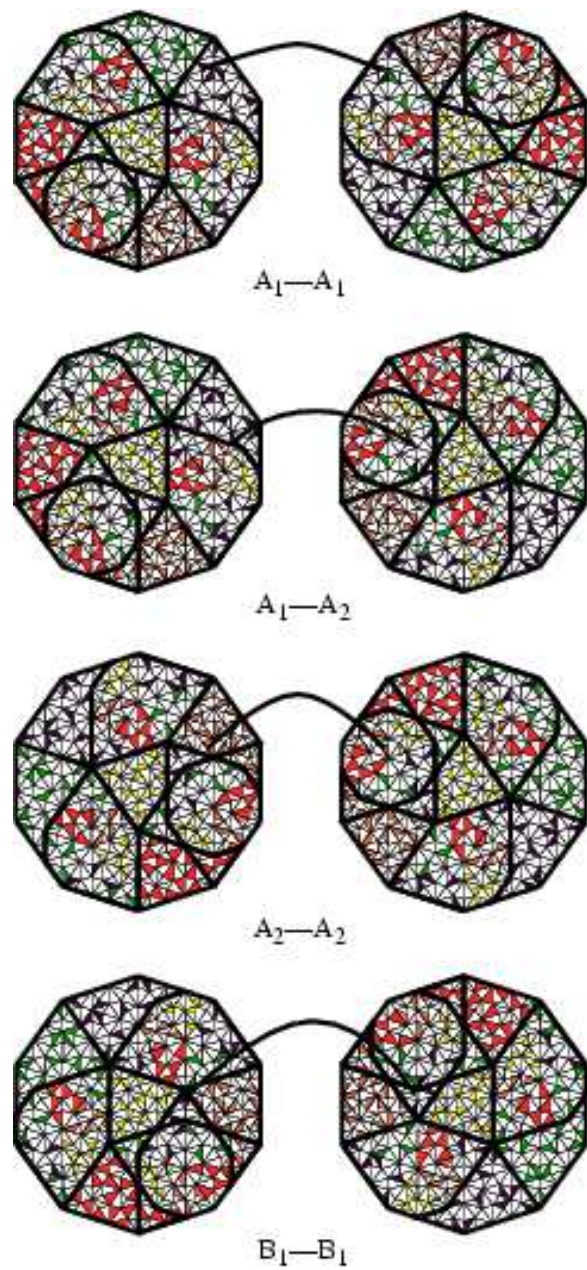
A_2—A_2

B_1—B_1

Figure 10: Locations of overlapping colored points in various representative illegal overlaps.
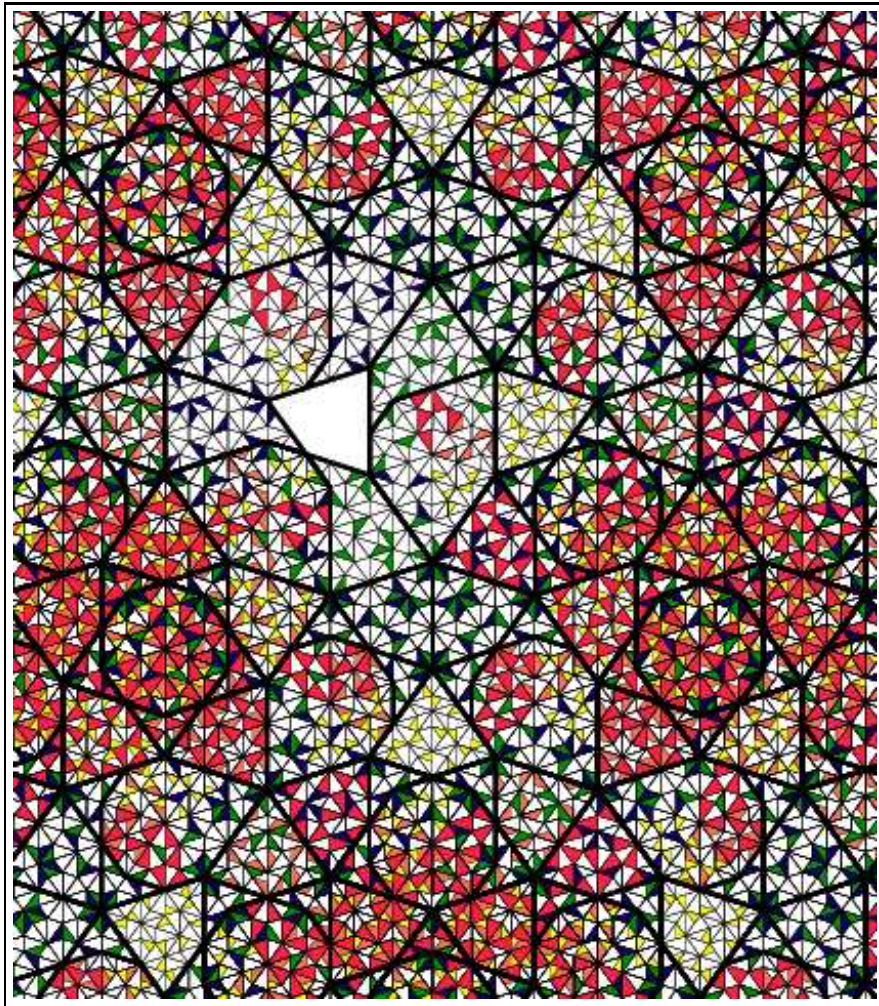
Figure 11: The beginnings of a consistent decagon tiling. The hole in the center can be covered with a tile in the obvious manner.

forth. The portion that remains in the limit $C'(I)$ is the set of all points of I that are mentioned by some interval of each step. For the interval $I = [l, r]$, the portion removed consists of

$$\mu(I \backslash C'(I)) = \left(\frac{1}{3} + \frac{1}{9} \cdot \frac{2}{3} + \frac{1}{27} \cdot \frac{8}{9} \cdot \frac{2}{3} + \cdots \right) \mu(I) \approx 0.44 \mu(I)$$

It follows, then, that the non-aggressive Cantor dust, $C'(I)$, saves $\sigma = 0.56$ of the measure $\mu(I)$. This positive measure set still enjoys many of the properties of the original Cantor set.[5] For example, the portion that is removed is dense within what remains. We now describe an important goal in our construction of Cantor-like sets:

Definition 5 *Two sets $S \subset I$ and $S^c = I \backslash S$ are* well mixed *if for any open interval $B \subseteq I$, $\mu(S \cap B) \neq 0$ and $\mu(S^c \cap B) \neq 0$.*

Well mixed sets are dense in each other and have positive measure everywhere. Since the set of Cantor dust that remains is not dense in the set that is removed (consider, for example, small open intervals centered in any interval removed) the two sets are obviously not well mixed. Indeed, the intervals removed work against the mixing. We now focus on post-processing the removed intervals.

As a basic step in our construction, we depend heavily on the non-aggressive Cantor construction on interval I, $C'(I)$. Notice that this construction is equivalent to computing $C'([0,1])$ and rescaling the result in the natural manner to fit within the interval $I = [l, r]$. In addition, the construction on an open or half-open interval differs from the construction on a closed interval by only one or two points.

	Construction of S_i			Area available	Area kept
0	S_0	$\longleftarrow C' \longleftarrow$	$R_0 = I$	$\mu(I)$	$\sigma \mu(I)$
1	S_1	$\longleftarrow C' \longleftarrow$	$R_1 = R_0 \backslash S_0$	$(1-\sigma)\mu(I)$	$\sigma(1-\sigma)\mu(I)$
2	S_2	$\longleftarrow C' \longleftarrow$	$R_2 = R_1 \backslash S_1$	$(1-\sigma)^2\mu(I)$	$\sigma(1-\sigma)^2\mu(I)$
$\vdots$					
i	S_i	$\longleftarrow C' \longleftarrow$	$R_i = R_{i-1} \backslash S_{i-1}$	$(1-\sigma)^i\mu(I)$	$\sigma(1-\sigma)^i\mu(I)$
$\vdots$					

Figure 12: A diagram guiding the construction of the approximants, S_i. Each stage involves applying a non-aggressive Cantor set operator (C') to the area available. The part removed is available for the next step.

We now develop a countable number of sets, S_i that, together, cover the points of interval $R_0 = I$. Figure 12 guides the process. First, let $S_0 = C'(I)$, a set with measure $\sigma\mu(I)$. This construction removed a countable number of open "remaindered" intervals, $R_1 = I \backslash S_0$ that have total measure $(1-\sigma)\mu(I)$. We hope to break up these remainders, to support the mixing. Thus, for $i > 0$ we define an *approximant*

$$S_i = \bigcup_{(a,b) \in R_i} C'((a,b))$$

This constructs dust from R_i with positive measure $\sigma(1-\sigma)^i\mu(I)$, and was derived by removing the countable open intervals

$$R_{i+1} = R_i \backslash S_i = I \backslash (S_0 \cup S_1 \cup \cdots \cup S_i)$$

with total measure $(1-\sigma)^{i+1}\mu(I)$.

---

[5]It is interesting to point out that while the middle-thirds Cantor construction $C(I)$ can be thought of as a composition of two sets that are similar to $C(I)$, that is not true for the non-aggressive construction, $C'(I)$.

The sets S_i are pairwise disjoint since they are defined on points of I remaindered from all previous steps. We may now define

$$S = \bigcup_{i=0}^{\infty} S_{2i}$$

and

$$S^* = \bigcup_{i=0}^{\infty} S_{2i+1}$$

Since the union operation here augments a Cantor set with dust from some of the removed area, this process is often called *refilling*. It is this refilling that eventually ensures the two sets are mixed. Sets S and S^* are disjoint, and avoid only a countable number of points in the original interval that correspond to endpoints a and b for each open interval removed during the Cantor set construction process. For our purposes, this countable collection of points is of marginal concern, and we note that these points augment S^* to provide:

$$S^c = I \backslash S$$

The two sets S and S^c, we claim, are well-mixed:

Theorem 6 *Suppose B is an open interval in I. Then $\mu(B \cap S) > 0$ and $\mu(B \cap S^c) > 0$.*

Proof: Note that $\mu(S) + \mu(S^c) = \mu(I)$ and that $\mu(B) > 0$. Since $\mu(S)$ and $\mu(S^c)$ are both positive we may assume that either $\mu(B \cap S)$ or $\mu(B \cap S^c)$ has positive measure. If neither were true, either B would be measure 0, or $\mu(S) + \mu(S^c) \le \mu(I \backslash B)$, both obvious contradictions. Without loss of generality, assume that $\mu(B \cap S) > 0$.

We will now show that $\mu(B \cap S^c) > 0$. Since $\mu(B \cap S)$ is positive there must be two points $l, r \in B \cap S$ such that $l < r$ and l and r are members of S_{2i} for some i. (There are only a countable number of S_{2i}, but $\mu(B \cap S) > 0$ which contains an uncountably infinite number of choices for l and r. Therefore there exists an S_{2i} such that $B \cap S_{2i}$ contains both l and r.) Since there are no open intervals contained within any S_{2i} there must be an open interval $J = (a, b)$ of diameter less than $r - l$ with $l < a < b < r$ such that J was removed during step $2i$. Clearly $J \subset B$. The Cantor operation on this interval, $C'(J)$, appears as a set of positive measure in $S_{2i+1} \subset S^*$. Furthermore, $\emptyset \subset (J \cap C'(J)) \subset (S^* \cap J)$. Thus $\mu(J \cap S^*) > 0$. That is to say $\mu(B \cap S^*) > 0$, or $\mu(B \cap S^c) > 0$. The theorem is thus proved. $\diamond$

It is simple to see, then, that S and S^c are well-mixed. While the two sets are disjoint, they are so interleaved that no open interval can be used to distinguish the two. Later we will use a related result to allow us to construct two non-overlapping point sets on a non-trivial open region similar to B.

We may compute the measure of S on interval I as

$$\mu(S) = \mu(I) \sum_{i=0}^{\infty} \sigma(1-\sigma)^{2i} = \frac{\sigma}{1 - (1-\sigma)^2} \mu(I) \approx 0.70 \mu(I)$$

The measure of the other set abides by the following relations:

$$\mu(I) - \mu(S) = \mu(S^c) = \mu(S^*) = \mu(I) \sum_{i=0}^{\infty} \sigma(1-\sigma)^{2i+1} = (1-\sigma)\mu(S) \approx 0.30\mu(I)$$

as we expect.

While we have constructed S (S^*) by accumulating the even (odd) numbered S_i, our theorem holds for any partitioning of the sets that leaves a countably infinite number in each of the two piles. As we shall see later, this can be used to achieve a measure for each of S and S^c that is arbitrarily close to equal division of the interval.

We note in passing that the notions of well-mixed sets may be extended to any finite number of sets using similar techniques. In particular:

Definition 7 *Suppose we are given n sets, $S(i)$, $0 \le i < n$ such that $I = \bigcup_{i=0}^{n} S(i)$. The sets are said to be well-mixed if for any open interval $B \subset I$, $\mu(B \cap S(i)) > 0$ for $0 \le i < n$.*

A collection of n sets might be constructed, for example, by accumulating the stepwise approximates, S_j, into sets in round-robin order, $0 \leq i < n$:

$$S(i) = \bigcup_{j=0}^{\infty} S_{nj+i}$$

Theorem 6 can be extended to demonstrate the well-mixed nature of these n sets.

In our next section, we make the analogy between open intervals and borderless Robinson tiles in $\mathbb{R}^2$.

3.2.2 The Well-Mixed Penrose Sponge

Our approach now is to construct different Cantor-like sponges from decomposed Robinson tilings. Each tile in a patch of Robinson tiles can be decomposed into similar tiles in a unique fashion. From this collection of subtiles we may elect to remove one or more leaving a portion of the original tile's decomposition. The remaining tiles are then decomposed in a similar manner with a percentage of the subtiles removed. The process can then, much in the manner suggested by Cantor, be repeated until a sponge-like structure is developed.

As with the Cantor set in $\mathbb{R}$, removal of a fixed percentage of the subtiles found in the decomposition can cause the remaining dust to have measure zero. We seek, then an analogous decreasingly aggressive removal process that leaves more "hefty" dust of positive measure.

A difficulty with this approach is that tiles are removed in quantum amounts. The percentage of the expanded tile removed depends on the number of decomposition steps that occur before subtiles are removed. For example, we know that, in the limit, large tiles cover approximately 62 percent ($\frac{1}{\tau}$) of the plane, while small tiles cover 38 percent ($1 - \frac{1}{\tau}$). Any finite number of decompositions of a single tile, however, only asymptotically (from above and below) approximates this ratio. Thus, as we remove tiles we seek to remove a target percentage with an error we may choose make as small as necessary at the cost of increasing the number of decomposition steps before tile removal.

Theorem 8 *Let f be the sequence of Fibonacci values, $0, 1, 1, 2, 3, 5, 8, \ldots$:*

$$f_i = \begin{cases} i & \text{if } i = 0 \text{ or } i = 1 \\ f_{i-2} + f_{i-1} & \text{if } i > 1 \end{cases}$$

After $d > 0$ decomposition steps,

1. *Robinson's S tile generates f_{2d-1} S subtiles and f_{2d} L subtiles.*

2. *Robinson's L tile generates f_{2d} S subtiles and f_{2d+1} L subtiles.*

The proof of this is derived with little effort by observing the self-similarity rules of Figure 7. With these ratios in hand, we can place bounds on the ratio, $r_d(P)$ of small to large subtiles that appear in the final decomposition.

Corollary 9 *Suppose we are given a finite patch P of tiles. After $d > 0$ decompositions, the ratio of S to L tiles, $r_d(P)$, meets the condition*

$$\frac{f_{2d}}{f_{2d+1}} \leq r_d(P) \leq \frac{f_{2d-1}}{f_{2d}}$$

with error not exceeding

$$\frac{f_{2d-1}}{f_{2d}} - \frac{f_{2d}}{f_{2d+1}} = \frac{1}{f_{2d}f_{2d+1}}$$

In addition, the percentage of the area occupied by S tiles after d decompositions approximates

$$\frac{1}{1 + \tau^2}$$

with error no greater than $5/\tau^{4d}$.

The endpoints of these estimations assume that P is composed of all L tiles (low) or all S tiles (high).

For the ease of controlling which subtiles are to be taken out after each decomposition, we define an *address* for each Robinson's tiles in the decomposition process. We denote Robinson's prototile types as we have elsewhere, with L and S tiles having left-handed versions denoted L' and S'. After decomposing a tile n times, we will obtain many subtiles, each identified by its containment in the stages of decomposition, read from left (before first decomposition) to right (after last decomposition). In Figure 13. The indicated tile is generated by decomposing Robinson's L tile three times: the tile resides in the S' tile that resulted from decomposing the L' tile, that resulted from decomposing the L' tile, that was a direct result of decomposing the original L. The address of the tile is, therefore, $LL'L'S'$. It is easy to see that there exists a bijection between the tile and its address.
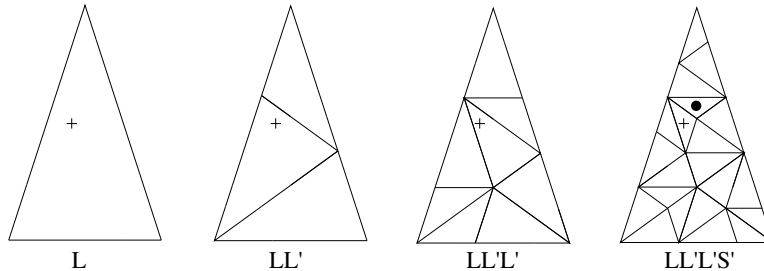

Figure 13: The address of the S tile marked with a $+$ in patch at right is $LL'L'S'$. Each step is one decomposition of the original L tile that determines the address of the tile. Note, also, that there is only one tile whose address ends in 3 S terms (marked with a $\bullet$): the one generated from the only small tile appearing after the first decomposition.

We are now prepared to algorithmically define the non-aggressive Cantor construction operation $K(P)$ on a patch of tiles P. Controlling the process is parameter d that determines the minimum number of decompositions that must occur at each step. As we have seen, above, increasing d will allow us to arbitrarily reduce the total error in our computation of the measure of the Cantor set.

We begin by decomposing P d times and removing all the small tiles—that is all tiles whose addresses end in one S. Since large tiles are τ larger than small tiles, the proportion, p_1, of the area that is occupied by these removed tiles, R_1, is:

$$\frac{f_{2d}}{f_{2d} + \tau f_{2d+1}} \leq p_1 \leq \frac{f_{2d-1}}{f_{2d-1} + \tau f_{2d}} \tag{1}$$

Let $P_1 = P \backslash R_1$. Patch P_1 is expanded $d+1$ times, and we remove the small tiles appearing as the result of directly decomposing small tiles—that is all tiles whose addresses end in two S's. These small tiles occupy a proportion p_2 of the remainder:

$$\frac{f_{2d}}{f_{2d} + \tau f_{2d+1}} \tau^{-2} \leq p_2 \leq \frac{f_{2d-1}}{f_{2d-1} + \tau f_{2d}} \tau^{-2}$$

since these small subtiles occupy exactly τ^{-2} of their small parents. The tiles removed, R_2, then, occupy $(1 - p_1)p_2$ percent of the original patch. This process continues by removing, more and more selectively, small tiles from what remains.

We can determine the measure of this set by approximating the amount removed. As d becomes large, the value of p_1 is brought arbitrarily close to $1/(1 + \tau^2)$, the percentage of area covered by small tiles in a complete tiling. We can simplify our analysis, then by approximating

$$p_i \approx \left(\frac{1}{1 + \tau^2} \right) \tau^{-2(i-1)}$$

Furthermore, since the term $\tau^{-2(i-1)}$ is exact the error due to whole tile removal is no greater than $5/(\tau^{4d+2i+1})$. Since the area kept is the result of not having been removed at any stage, the area that

remains is

$$\mu(P)\prod_{i=0}^{\infty}\left(1-\left(\frac{1}{1+\tau^2}\right)\tau^{-2i}\right)$$

This latter expression is not easy to simplify, but converges quickly to $\rho\mu(P)$, where $\rho = 0.605741$. Thus, the $K(P)$ operation leaves approximately 61 percent of the tile intact. The error in ρ is bounded by the worst cases of consistently overestimating and consistently underestimating the amount removed at each stage, and has total error no worse than

$$\mu(P)\sum_{i=1}^{\infty}\frac{5}{\tau^{4d+2i+1}} = \frac{5}{\tau^{4d+2}}\mu(P)$$

Notice that $P - K(P)$ is a countable collection of open, S tiles. This set is dense in $K(P)$, but the opposite is not true. To achieve mixing, as in the one dimensional case, we refill each of the small tiles with the appropriate K construction on those tiles. We set $R_0 = P$, and compute $S_0 = K(R_0)$. This set has measure $\rho\mu(P)$ and the remainder, $R_1 = R_0 \backslash S_0$, has $(1-\rho)\mu(P)$. At each stage, S_i is the result of applying K to the remainder set R_i generated by the previous step. $S_i = K(R_i)$ has measure $\rho(1-\rho)^i\mu(P)$, and each remainder has measure $(1-\rho)^i\mu(P)$.

In a round-robin manner described before for patch P and $0 \le i < 5$ the well-mixed set representing color i is

$$S(i) = \bigcup_{k=0}^{\infty} S_{5k+i}(P)$$

The measures of these sponges are easily computed, as

$$\mu(S(i)) = \sum_{k=0}^{\infty}\mu(S_{5k+i}(P)) = \sum_{k=0}^{\infty}\rho(1-\rho)^{5k+i}\mu(P) = \frac{\rho(1-\rho)^i}{1-(1-\rho)^5}\mu(P)$$

This round-robin distribution of sets sponges among the colors is not very equitable: sponge 0 takes up 61 percent, while sponge 4 accounts for 1.5 percent of the patches they appear in. Still these sponges are well mixed:

Theorem 10 *Suppose B is an open interval in P. Then $\mu(B \cap S(i)) > 0$ for all $0 \le i < 5$.*

Since the sponges sum to $\mu(P)$ (save measure zero edges dropped in the K construction) and since B is open, $\mu(B \cap S(i)) > 0$ for some i, say, without loss of generality, it is 0. It is also clear that there is a disc $D \subseteq (B \cap P)$ such that $D \subseteq P_{5k}$ (there are only a countably infinite number of such sets, and they, in total, make up $S(0)$). Within D there must be an open, S tile shaped region, B_1 that was removed during step $5k$. Clearly, $B_1 \subseteq B$ and $K(B_1)$ (which has measure $\rho\mu(B_1)$) was included in the construction of $P_{5k+1} \subset B \cap S(1)$, so $\mu(B \cap S(1)) > 0$. Iterating this process leads to similar conclusions about the remaining sponges, $S(2)$, $S(3)$, and $S(4)$.◇

We have, then, a means of constructing five different sponges that intermingle without overlap, with the additional advantage that each sponge appears with significant measure at all locations. Our second, heftier decagon, is constructed using points from these equivalence classes and inherits the same edges and matching rules from the lacy construction.

While the five sponges can be used to cover a patch, fewer than five tiles overlap in a single region. In these areas, a significant measure of points is not covered (corresponding to colors missing in the region). This seems to be an essential difficulty with the approach, although any point that is not covered is, of course, surrounded arbitrarily closely by points that are covered by each of the participating colors.

The general approach to developing porous tiles from overlapping shapes should, of course, generalize to higher dimensions. One difficulty, of course, is the development of overlapping polyhedra that cover the space in an appropriate manner. It should be noted, however, that while two colors (black and clear) were sufficient for Gummelt's decagon, one might imagine a coloring of regions of a polyhedron from a larger selection of colors. These colors would then be transformed into interleaved sponges that support or reject particular overlaps.

3.2.3 Balancing Sponge Measures

In our hefty decagon we constructed sponges that are positive measure everywhere. One unfortunate feature is that their measures are dramatically different. Aside from being aesthetically unappealing, the ability to control the density of the different sponges may lead to more realistic models of interactions in physical systems. Here, we demonstrate that a first-fit bin-packing algorithm is sufficient to generate sponges with densities that are equal.

We start with five bins, b_i $0 \leq i < 5$, each with capacity 0.2. Ultimately each bin will hold the approximants that will determine the component sponges of one color set. During our construction, $\rho > 0.2$ so P_1 will not fit within any bin. We modify, then, our K operation so that instead of removing S tiles, we remove tiles according to the number of L's in the tile address. This results in a proportion of $\rho_L = 0.0146634$ and, $\mu(P_0) = 0.0157$, $\mu(P_1) = 0.0154$, $\mu(P_2) = 0.0152$, ...

The bin-packing algorithm assigns the measure of each point set into an appropriate bin in a first-fit fashion:

PackBins:
    $i \leftarrow 0$
    do forever
        $j \leftarrow 0$
        while $(\mu(b_j) + \mu(P_i) \geq 0.2)$
            $j \leftarrow j + 1$
        end
        add set P_i to bin b_j
        $i \leftarrow i + 1$
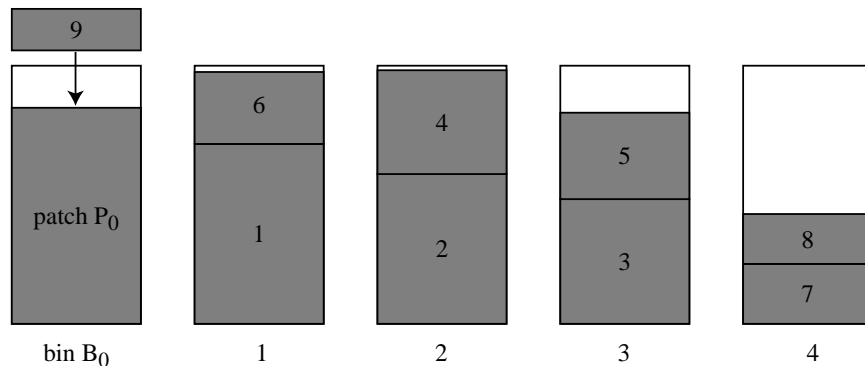   **end**
  end

Figure 14: Allocating patches to groups by packing bins. Patch P_9 is placed in the first bin that has room, bin 0. In this figure, patches are scaled assuming we remove only one of two L tiles in the Cantor step; in the text the patches are smaller since we remove two L tiles.

In order for the algorithm to generate sponges with perfectly balanced measures, we need to ensure two things. First, the inner loop in the algorithm can always exit before $j = 5$. In the ith step, we are trying to find a slot in one of the bins to accommodate 1.57% of the total unfilled area. Since we have 5 bins, there is at least one bin whose unfilled area is no less than 20% of the total unfilled area. Therefore, we are always able to find such a slot. As a result, the inner loop will always exit before $j = 5$.

Second, no bin is ever completely filled during the iterations; each bin will be filled by an infinite number of point sets. The condition $\mu(b_j) + \mu(P_i) \geq 0.2$ effectively prevents any bins from being completely filled during our iterations. For the proof of well mixing to work, we must be able to, at any stage in the bin packing process, be assured that we will place a set in each of the five bins within a finite number of steps.

There is, of course, nothing special about the relative sizes of the bins. If colors could be consistently aligned with regions of influence in a physical quasicrystal, their relative densities could be adjusted to better reflect, say the degree of influence on neighboring unit cells.

4   Conclusions

It is, of course, always intriguing to develop a shape with aperiodic behavior. We have found the overlapping nature of the decagon tile has been useful in two distinct respects. First, it seems that physical systems with decagonal long-range symmetry are more adequately modeled if we allow this overlap. The interpretation of the overlap is the sharing of molecular regions in a unit cell. Secondly, we believe the use of overlap has served as a catalyst to better understand how other nontraditional tile shapes interact aperiodically.

In the prototiles presented here we demonstrate how to use the inflation-based similarities of tiles to construct dense tiling by a single prototile that is either zero measure or positive measure everywhere. In the constructions presented here, formal matching rules include interior and exterior edges that must meet in the manner inherited from the decagon cover. These edges are clearly necessary in the lacy tile that covers almost nowhere. It is not known, however, whether these edge rules are strictly necessary in the heftier constructions, where the overlapping sponges may inherit the interlocking geometry of the self-similar decompositions.

We also demonstrate how to adjust the relative densities of tile regions, perhaps to more accurately model the influence of physical quasicrystal systems. Recent work by Jeong and Steinhardt[13] has studied the stoichiometry of the unit cells of quasicrystals with 10-fold long-range symmetry, and is greatly facilitated by the decagon tiling and its offshoots. Their techniques compute precise densities of atoms per unit area of the crystal. It seems likely that the simplicity of the equal-density construction of Section 3.2.3 would be suitable for many purposes, though other density distributions are possible.

References

[1] Robert Ammann, Branko Grünbaum, and G. C. Shephard. Aperiodic tiles. *Discrete and Computational Geometry*, 8:1–25, 1992.

[2] C. Bandt and Petra Gummelt. Fractal Penrose tilings I: Construction and matching rules. *Aequationes Mathematicae*, 53:295–307, 1997.

[3] Robert Berger. The undecidability of the domino problem. *Memoirs of the American Mathematical Society*, 66, 1966.

[4] N. G. de Bruijn. Algebraic theory of Penrose's non-periodic tilings. *Nederl. Akad. Wetensch. Proc.*, 84:39–66, 1981.

[5] N. G. de Bruijn. Updown generation of Penrose patterns. *Indagationes Mathematicæ*, 1(2):201–220, 1990.

[6] Martin Gardner. Extraordinary nonperiodic tiling that enriches the theory of tiles. *Scientific American*, pages 110–121, January 1977.

[7] Götz Gelbrich. Fractal Penrose tiles II: Tiles with fractal boundary as duals of Penrose triangles. *Aequationes Mathematicæ*, 54:108–116, 1997.

[8] Michael Goldberg. Central tessellations. *Scripta Mathematica*, 21:253–260, 1955.

[9] Branko Grünbaum and G. C. Shephard. Is there an all-purpose tile? *The American Mathematical Monthly*, 93:545–551, August/September 1986.

[10] Branko Grünbaum and G. C. Shephard. *Tilings and Patterns*, chapter 10. W. H. Freeman and Company, New York, 1987.

[11] Petra Gummelt. Penrose tilings as coverings of congruent decagons. *Geometriae Dedicata*, 62(1):1–17, August 1996.

[12] Hyeong-Chai Jeong and Paul Steinhardt. Constructing Penrose-like tilings from a single prototile and the implications for quasicrystals. *Physical Review B*, 55(6):3520–3532, February 1997.

[13] Hyeong-Chai Jeong and Paul J. Steinhardt. Rules for computing symmetry, density and stoichiometry in a quasi-unit-cell model of quasicrystals. Technical Report 9901014, arXiv ePrint, December 2002.

[14] Richard Klitzing and Michael Baake. Representation of certain self-similar quasiperiodic tilings with perfect matching rules by discrete point sets. *Journal de Physique I*, 4:893–904, 1994.

[15] J. C. Lagarias. Geometric models for quasicrystals I: Delone sets of finite type. *Discrete and Computational Geometry*, 21:161–191, 1999.

[16] J. C. Lagarias. Geometric models for quasicrystals II: Local rules under isometries. *Discrete and Computational Geometry*, 21:345–372, 1999.

[17] Dov Levine and Paul J. Steinhardt. Quasicrystals. I. definition and structure. *Physical Review B*, 34(2):596–616, July 1986.

[18] George Y. Onoda, Paul J. Steinhardt, David P. DiVincenzo, and Joshua E. S. Socolar. Growing perfect quasicrystals. *Physical Review Letters*, 60(25):2653–2656, June 1988.

[19] R. Penrose. The rôle of aesthetics in pure and applied mathematical research. *Bulletin of the Institute of Mathematics and Its Applications*, 10:266–271, 1974.

[20] R. Penrose. *Pentaplexity: A class of non-periodic tilings of the plane*, chapter 5, pages 55–65. Pitman, Boston, 1984.

[21] E. Arthur Robinson, Jr. The dynamical properties of Penrose tilings. *Transactions of the American Mathematical Society*, 348(11):4447–4464, November 1996.

[22] Marjorie Senechal. *Quasicrystals and Geometry*. Cambridge University Press, Cambridge, 1995.

[23] Cesar Silva. *Invitation to Ergodic Theory*. Manuscript in progress, 2001.

[24] Joshua E. S. Socolar and Paul J. Steinhardt. Quasicrystals. II. unit-cell configurations. *Physical Review B*, 34(2):617–647, July 1986.

[25] Hao Wang. Games, logic, and computers. *Scientific American*, pages 98–106, November 1965.

[26] Feng Zhu. The search for a universal tile. Technical report, Williams College Department of Computer Science, 2002.